Microbiological Research 241 (2020) 126592

Contents lists available at ScienceDirect

Microbiological Research

journal homepage: www.elsevier.com/locate/micres

The *stuA* gene controls development, adaptation, stress tolerance, and virulence of the dermatophyte *Trichophyton rubrum*

Elza A.S. Lang [a], Tamires A. Bitencourt [a], Nalu T.A. Peres [b], Lucia Lopes [a], Larissa G. Silva [a], Rodrigo A. Cazzaniga [a], Antonio Rossi [a], Nilce M. Martinez-Rossi [a,*]

[a] Department of Genetics, Ribeirão Preto Medical School, University of São Paulo, Ribeirão Preto, São Paulo, Brazil
[b] Department of Microbiology, Institute of Biological Sciences, Federal University of Minas Gerais, Belo Horizonte, Brazil

ARTICLE INFO

Keywords:
APSES domain
Keratinocytes
StuA
Host-pathogen interaction
Stress resistance
Mechanosensing

ABSTRACT

The APSES family, comprising of the transcriptional regulators Asm1p, Phd1p, Sok2p, Efg1p, and StuA, is found exclusively in fungi and has been reported to control several cellular processes in these organisms. However, its function in dermatophytes has not yet been completely understood. Here, we generated two null mutant strains by deleting the *stuA* gene in the dermatophyte *Trichophyton rubrum*, the most common clinical isolate obtained from human skin and nail mycoses. The functional characterization of the knocked-out strains revealed the involvement of *stuA* in germination, morphogenesis of conidia and hyphae, pigmentation, stress responses, and virulence. Although the mutant strains could grow under several nutritional conditions, growth on the keratin medium, human nails, and skin was impaired. The co-culture of *stuA* mutants with human keratinocytes revealed enhanced development. Moreover, a *stuA* mutant grown on the keratin substrate showed a marked decrease in the transcript numbers of the hydrophobin encoding gene (*hypA*), suggesting the involvement of *stuA* in the molecular mechanisms underlying mechanosensing during the fungi-host interaction. In addition, bioinformatics analyses revealed the potential involvement of StuA in different biological processes such as oxidation-reduction, phosphorylation, proteolysis, transcription/translation regulation, and carbohydrate metabolism. Cumulatively, the present study suggested that *StuA* is a crosstalk mediator of many pathways and is an integral component of the infection process, implying that it could be a potential target for antifungal therapy.

1. Introduction

Successful fungal pathogenesis depends on the adaptive processes that allow the fungus to install itself and survive in the host (Hogan et al., 1996; Martinez-Rossi et al., 2012, 2017). Dermatophytes infect keratinized tissues, such as hair, nails, and skin, and secrete enzymes that degrade these substrates providing the nutrients. Keratin is an insoluble protein rich in cysteine, and the ability of the fungus to degrade this substrate, mediated by keratinases, contributes to its survival and pathogenicity (Viani et al., 2001; Vermout et al., 2008).

Studies using *ex vivo* infection models have shown that the degradation of keratin by dermatophytes relies on the secretion of sulfite, which helps in the cleavage of keratin-stabilizing cystine bonds (Grumbt et al., 2013). Molecular studies using different infection models in the zoophilic and anthropophilic dermatophytes *Arthroderma benhamiae* and *Trichophyton rubrum*, respectively, have generated insights into the molecular mechanisms underlying dermatophyte-host interactions (Staib et al., 2010; Mehul et al., 2016; Peres et al., 2016; Tran et al., 2016). Of the several keratin-degrading dermatophytes, *T. rubrum* has been reported to be one of the most prevalent causative agents of human dermatophytosis, and responsible for the majority of clinical cases of superficial mycoses of skin and nail.

Transcription factors participate in many cellular processes, including virulence and pathogenicity. The APSES family of transcriptional regulators belongs to the basic-helix-loop-helix (bHLH) class of transcription factors and is ubiquitous in several fungi (Zhao et al., 2015). APSES is an acronym of Asm1p, Phd1p, Sok2p, Efg1p, and StuA proteins that carry a conserved DNA binding domain, the APSES domain, earlier described in the fungi *Neurospora crassa* (Asm1p), *Saccharomyces cerevisiae* (Phd1p and Sok2p), *Candida albicans* (Efg1p),

Abbreviations: WT, wild type; *hypA*, hydrophobin encoding gene; MM, minimal media; MEA, malt extract agar; SAB, Sabouraud; PDA, potato dextrose agar; FBS, fetal bovine serum; CFUs, colony forming units; UV, ultraviolet; RT-PCR, real-time PCR.

* Corresponding author at: Department of Genetics, Ribeirão Preto Medical School, University of São Paulo, 14049-900, Ribeirão Preto, São Paulo, Brazil.
E-mail address: nmmrossi@usp.br (N.M. Martinez-Rossi).

https://doi.org/10.1016/j.micres.2020.126592
Received 11 April 2020; Received in revised form 29 August 2020; Accepted 11 September 2020
Available online 18 September 2020

and *Aspergillus nidulans* (StuAp) (Gimeno and Fink, 1994; Aramayo et al., 1996; Dutton et al., 1997; Stoldt et al., 1997b). The APSES transcription factors participate in controlling several processes, such as cell differentiation, spore germination, mycelial growth, sporulation, virulence, pathogenicity, dimorphic growth, sexual reproduction, primary and secondary metabolism, and fungal development, in different fungi (Zhao et al., 2015).

However, the role of APSES regulators may vary among different species. The APSES regulator Asm1 is involved in conidial germination, aerial hyphae growth, and sexual and asexual development in *N. crassa*, and is thus required for protoperithecia formation (Aramayo et al., 1996). In *C. albicans*, the APSES protein Efg1p is involved in several morphogenetic processes, such as yeast-to-hypha transition, chlamydospore formation, cell shape determination during white-opaque switching, and biofilm formation (Stoldt et al., 1997a; Sonneborn et al., 1999; Srikantha et al., 2000; Ramage et al., 2002). In *A. nidulans*, the APSES protein StuAp regulates sexual and asexual reproduction important for conidiophore formation and other morphogenetic processes. StuAp also binds to the StuAp response elements, with the consensus 5′-(A/T)CGCG(T/A)N(A/C)-3′ at the promoter regions of target genes (Dutton et al., 1997; Wu and Miller, 1997). In *Stagonospora nodorum*, StuA regulates the central carbon metabolism, and the deletion of *stuA* has been shown to affect glycolysis, TCA cycle, and amino acid synthesis (IpCho et al., 2010). Moreover, StuA deletion impairs the virulence of phytopathogens *Glomerella cingulata*, *Magnaporthe grisea*, *S. nodorum*, and *Fusarium graminearum* (Tong et al., 2007; Nishimura et al., 2009; IpCho et al., 2010; Lysoe et al., 2011). StuA is also involved in the generation of normal turgor pressure within the appressorium of *G. cingulata* necessary for the formation of the penetration peg (Tong et al., 2007). Although StuA is not required for the process of infection in human pathogens, *A. fumigatus* and *H. capsulatum* (Sheppard et al., 2005; Longo et al., 2018), it is required for the development of mycelial traps for nematode capture and the production of extracellular enzymes necessary for the degradation of nematode cuticle, allowing fungal penetration and infection in the nematophagous fungus *Arthrobotrys oligospora* (Xie et al., 2019). Furthermore, StuA is involved in keratin degradation and sexual reproduction in the dermatophyte *Arthroderma benhamiae* (Krober et al., 2017). In this study, we evaluated the role of the *stuA* gene in development, interaction with host molecules and tissues, tolerance to adverse environmental conditions, and virulence of *T. rubrum*. The role of the gene was confirmed by developing two *stuA* mutant strains.

2. Materials and methods

2.1. T. rubrum strains and culture conditions

T. rubrum strain CBS118892 (CBS-KNAW Fungal Biodiversity Centre) was used as the wild-type (WT) strain in this work to generate Δ*stuA*(1) and Δ*stuA*(2) mutants. The strains were grown at 28 °C in malt extract agar [MEA: 2% glucose (w/v), 2% malt extract (w/v), 0.1 % peptone (w/v), pH 5.7], Sabouraud [SAB: 2% glucose (w/v), 1% peptone (w/v), pH 5.7], minimal medium (MM) (Cove, 1966) pH 5.0, potato dextrose agar [PDA: 0.4 % potato extract (w/v), 2% dextrose (w/v), pH 5.7], or keratin medium [0.25 % keratin powder (w/v) - MP Biomedicals, pH 5.5]. Solid media contained 2% agar (w/v). Conidia suspensions were obtained by harvesting 21-days-old cultures grown on MEA, and conidia concentrations were estimated by counting in the Neubauer chamber, as previously described (Jacob et al., 2015).

2.2. Human keratinocytes and culture conditions

The HaCat keratinocyte cell line was cultured in RPMI medium (Sigma-Aldrich), supplemented with 10 % (v/v) fetal bovine serum (FBS) (Cult lab, Brazil), at 37 °C in a humidified atmosphere with 5% CO_2, as previously described (Komoto et al., 2015)

2.3. In silico analyses

The *stuA* gene with the accession number TERG_00714 (https://www.ncbi.nlm.nih.gov/gene/10374520) was retrieved from the genome database of *T. rubrum* CBS118892. The annotated protein (accession number XP_003238727.1) was used in BLASTP (https://blast.ncbi.nlm.nih.gov/Blast.cgi?PAGE=Proteins) analyses to search for orthologs.

The accession numbers of selected *T. rubrum stuA* orthologs were as follows: *N. crassa* (AAB06995.1), *M. grisea* (Q4R1B9.1), *A. nidulans* (CBF70741.1) *A. fumigatus* (Q4 × 228.1), *Microsporum gypseum* (EFQ97814.1), *T. interdigitale* (EZF28392), *T. tonsurans* (EGD94730.1), *T. equinum* (EGE03647.1), and *A. benhamiae* (XP_003013983). Functional protein domains were analyzed with InterProScan sequence search (http://www.ebi.ac.uk/interpro/search/sequence-search) and ScanProsite (http://prosite.expasy.org/scanprosite/) tools. Sequences were aligned with Clustal Omega multiple sequence alignment tool (https://www.ebi.ac.uk/Tools/msa/clustalo/) and shaded by the BoxShade server (http://www.ch.embnet.org/software/BOX_form.html).

2.4. stuA transcription profile

Approximately 10^6 WT conidia were inoculated in 100-ml keratin broth, which was incubated at 28 °C under shaking at 100 rpm for 48 h, 72 h, and 96 h. Mycelia were collected by filtration, and total RNA was extracted using the Illustra RNAspin Isolation Kit (GE Healthcare Life Sciences). RNA was treated with DNase I Amplification Grade (Thermo Fisher Scientific) and used for cDNA synthesis with a High Capacity cDNA Synthesis kit (Thermo Fisher Scientific). qPCR reactions were conducted using SYBR green PCR master mix (Thermo Fisher Scientific) and StepOnePlus Real-time PCR System (Thermo Fisher Scientific), as previously described (Jacob et al., 2015). For these reactions, 100 ng of cDNA, 600 nM of *hypA* primers, and 600 nM of *stuA* primers (S1 and S2) were used. Data were normalized using the *rpb2* gene as the reference, as previously described (Jacob et al., 2012). Relative expression was calculated using the $2^{-\Delta\Delta CT}$ method (Livak and Schmittgen, 2001). All primers used in this study are listed in Supplementary Table S1.

2.5. stuA gene deletion

Double-joint PCR (Yu et al., 2004) and split-marker (Catlett et al., 2003) approaches were used in this work to generate the gene-replacement constructs. Briefly, *stuA* 5′ and 3′ flanking regions (1.7 kb and 1.9 kb, respectively) were amplified with primers P1 and P2 and with P3 and P4, respectively. A 2.6-kb fragment containing the hygromycin B phosphotransferase (*hph*) gene, under the control of the promoter and terminator of the *A. nidulans trpC* gene, was amplified by PCR from pCSN43 plasmid (Fungal Genetics Stock Center), with primers M13_F and M13_R. Primers P2 and P3 have tails complementary to the primers M13_F and M13_R, respectively. Next, *stuA* 5′ and 3′ flanking fragments and *hph* cassette were mixed and fused by double-joint PCR (Yu et al., 2004), and the product was then used as the template to amplify split-marker fragments (Catlett et al., 2003) with primers P5 and H1 and with H2 and P6, generating fragments of 2.8 kb and 3.8 kb with an overlapping region of approximately 400 bp. All PCR reactions were performed using Platinum Taq DNA Polymerase High Fidelity (Thermo Fisher Scientific) and purified using the Wizard SV Gel and PCR Clean-up System (Promega). Split-marker fragments were co-transformed into *T. rubrum* WT protoplasts.

To obtain protoplasts, we inoculated approximately 10^9 WT conidia into 100 ml SAB broth and incubated it at 28 °C under shaking (100 rpm) for 48 h. The resulting mycelia were transferred to 25 ml of lytic solution (1.1 M KCl, 0.1 M citric acid, 4 mg/ml lysing enzymes from *Trichoderma harzianum* [Sigma-Aldrich], 4 mg/ml lysozyme, 4 mg/ml bovine serum albumin, pH 5.8), and incubated at 30 °C and 100 rpm for approximately 4−5 h. Protoplasts were filtered through glass wool, washed twice with

25 ml of the STC buffer (1.2 M sorbitol, 50 mM Tris, 10 mM $CaCl_2$, pH 7.5), collected by centrifugation (2000 × *g*, 10 min), and then resuspended in 1 ml of STC buffer. For protoplast transformation, split-marker fragments (10 μg in 100 μl of STC buffer) were added to 100 μl of protoplast suspension and incubated at 25 °C for 20 min, followed by the addition of 1 ml polyethylene glycol solution [25 % PEG 6000 (w/v) in STC buffer] and incubation at 25 °C for 20 min. No DNA was added to the negative controls. Transformants were selected on solid SAB supplemented with 1.2 M sorbitol and 450-g ml^{-1} hygromycin B after incubation at 28 °C for 15 days.

2.6. Identification of *stuA* null mutants

To identify *stuA* null mutants, the transformants grown in hygromycin B were screened using PCR and Southern blot analyses. Briefly, genomic DNA was isolated by grinding fresh mycelia in the presence of extraction solution [5 mM EDTA, 1% SDS (w/v), pH 8.0], followed by incubation at 68 °C for 10 min and centrifugation at 11,000 × g for 5 min. The supernatant was collected, and 200 mM potassium acetate was added, followed by incubation on ice for 1 h and centrifugation (5 min, 11,000 × g). The supernatant was subjected to phenol/chloroform extraction, followed by precipitation with ethanol, two steps of washing with 70 % ethanol, and drying. The precipitate was resuspended in a buffer comprising 1 mM EDTA and 10 mM Tris−HCl (pH 7.5) as well as RNase A (50 μg ml^{-1}), followed by incubation at 65 °C for 10 min. Isolated DNA was used in molecular analyses.

For mutant screening by PCR, genomic DNA from WT and transformants was tested for both the amplification of a 143-bp internal region of *stuA* gene with primers S1 and S2 and amplification with primers P1 and P4, with the generation of distinct sizes for WT and *stuA* mutants (5.6 kb and 6.3 kb, respectively). Southern blot hybridizations were then used for verifying potential *stuA* mutants. Genomic DNA from WT and selected transformants were cleaved with EcoRI and BamHI and probed using a 0.7-kb fragment of *stuA* 3′ flanking region to detect an expected fragment of 6.1 kb for the WT or 2.8 kb for *stuA* mutants. Genomic DNAs were also cleaved with BglII and BclI and probed with the *hph* cassette to detect an expected fragment of 6.2 kb in *stuA* mutants and no fragment in WT. The DIG-High Prime DNA Labeling and Detection Starter Kit II (Roche) was used for labeling and detection. So, the deletion of the *stuA* gene and integration of the *hph* gene was confirmed by PCR and Southern blot analysis.

2.7. Growth, morphology, hydrophobicity, and germination tests

To evaluate colony growth and morphology, mycelia plugs of approximately 2 mm in diameter from WT, Δ*stuA*(1), and Δ*stuA*(2) strains were inoculated onto the center of MEA, SAB, PDA, MM, or keratin media (150 × 15 mm Petri dishes), and incubated at 28 °C for 21 days. Front and reverse sides of the colonies were photographed, and the colony radial extension was evaluated by measuring colony diameter.

For side view of the colonies, a rectangular block (height × length × width, 1 × 2 × 1 cm) of either MEA or SAB solid media was placed between 2 microscope slides. Then a mycelial plug was inoculated on the center of one of the most massive lateral faces of the block. The "sandwich" was incubated at 28 °C for 5 days in a humid chamber kept in a closed Petri dish and was photographed against the light to visualize aerial and vegetative hyphae.

Mycelia hydrophobicity was tested, as previously described (Heddergott et al., 2012), by dropping 50 μl of either water or 0.005 % bromophenol blue solution (w/v) onto 21 day-old mycelia from WT, Δ*stuA*(1), and Δ*stuA*(2) strains grown on MEA or SAB solid media.

Microscopic aspects of hyphae and conidia were assessed by slide culture (Harris, 1986). Cubes (1 cm^3) of MEA media on water agar plates were inoculated with mycelia plugs on all lateral faces, overlaid by coverslips, and incubated at 28 °C for 14 days. The coverslips were then used in lactophenol cotton blue slide mounting followed by light microscopy imaging.

To analyze germination, we inoculated 6-well plates containing 10 ml SAB broth per well with approximately 10^5 conidia, followed by incubation at 28 °C. After 3 h and 20 h, the plates were assessed using light microscopy imaging.

2.8. Ex vivo infection of human nail and skin

Human fingernail fragments were obtained from healthy donors, autoclaved, and placed on water agar plates, as previously described (Grumbt et al., 2013). Then they were inoculated with the conidia from WT, Δ*stuA*(1), or Δ*stuA*(2) strains (3 × 10^5 conidia per fragment). After 30 days of incubation at 28 °C, nails were photographed and analyzed by scanning electron microscopy.

Human skin fragments were obtained from healthy donors who underwent plastic surgery at the Clinics Hospital of Ribeirão Preto Medical School, University of São Paulo, and used for infection experiments, as previously described (Peres et al., 2016). Briefly, after removing the adipose tissue, small skin fragments (1 cm^2) on a thin layer of Skin Graft Fluid (Duek et al., 2004) were inoculated with conidia from WT, Δ*stuA* (1), or Δ*stuA*(2) strains (10^4 conidia per fragment) and incubated at 28 °C in closed Petri dishes in a humid chamber. After 96 h, skin fragments were analyzed by scanning electron microscopy.

All procedures were conducted in agreement with the Ribeirão Preto Medical School Ethics Committee approval (protocol number 8330/2009).

2.9. Co-culture of *T. rubrum* and human keratinocytes

HaCat human keratinocytes were co-cultured with *T. rubrum* conidia, as previously described (Bitencourt et al., 2020). Briefly, keratinocytes were seeded in a 25-cm^2 tissue culture flask at a density of 2.5 × 10^5 cells ml^{-1} and grown in RPMI supplemented with 5% FBS (v/v) for 24 h at 37 °C in a humidified atmosphere with 5% CO_2. Next, conidia from WT, Δ*stuA*(1), and Δ*stuA*(2) strains, previously suspended in RPMI supplemented with 5% FBS (v/v), were added to the keratinocytes cultures (10^6 conidia ml^{-1}) and incubated at 37 °C with 5% CO_2 for 24 h. The resulting co-cultures were evaluated by light microscopy after May--Grünwald-Giemsa staining.

2.10. Keratinolytic activity

Approximately 5 × 10^5 conidia from WT, Δ*stuA*(1), and Δ*stuA*(2) strains were inoculated into 50 ml keratin broth and incubated at 28 °C under shaking at 100 rpm for 96 h. The pH of the culture media was measured before and after cultivation. Mycelia were collected by filtration to measure the dry weight, and crude culture supernatants were immediately used in enzymatic assays. For each reaction, 20 mg of keratin powder (MP Biomedicals) suspended in 4 ml of 28 mM Tris−HCl buffer (pH 8.0) was used as the substrate for 1 ml of culture supernatant. The enzymatic reactions were conducted at 45 °C for 30 min and 160 rpm. Keratinolytic activities (units per gram of mycelia dry weight) were determined as previously described (Ferreira-Nozawa et al., 2006).

2.11. Microscopy

Light microscopy imaging was performed using a Leica DMI3000B inverted microscope. For scanning electron microscopy, samples were fixed with 3% glutaraldehyde in 0.1 % phosphate buffer (v/v) (pH 7.2) at 4 °C for 2 h, rinsed with 0.1 % phosphate buffer (pH 7.2), and post-fixed with 1% osmium tetroxide for 2 h, followed by dehydration using a graded ethanol series. Samples were then sputter-coated with gold and viewed under a Jeol JSM-6610 LV scanning electron microscope at an acceleration voltage of 25 kV.

2.12. Heat-shock and UV light exposure

Conidia suspensions from WT, Δ*stuA*(1), and Δ*stuA*(2) strains were submitted to heat-shock and UV light exposure. For heat-shock tests, tubes containing 1 ml of conidia suspension (10^5 conidia ml^{-1}) were incubated in a water bath at 42 °C for 30 and 60 min, with shaking and plated on solid SAB. After incubation at 28 °C for 5 days, colony-forming units (CFUs) were counted. For UV light exposure, 5 ml of conidia suspension (10^5 conidia ml^{-1}) in opened plastic Petri dishes were irradiated with UV germicidal light (G1578 UV lamp) at 16 cm distance for 15 s with constant shaking and were plated on solid SAB. After incubation at 28 °C in the dark for 5 days, CFUs were counted. As controls, CFUs from untreated conidia were counted. Relative survival was the percentage of CFUs from treated conidia relative to the CFUs from untreated conidia.

2.13. Statistical analyses of experimental data

Results were presented as mean values from independent experiments ± standard deviations. Statistically significant differences were determined by one-way analysis of variance followed by Bonferroni's multiple comparison tests, using the GraphPad Prism 5 Software.

3. Results

3.1. Identification of stuA gene in T. rubrum

The ortholog of the *stuA* gene was identified from the genome database of *T. rubrum* CBS 118892 (https://www.ncbi.nlm.nih.gov/gene/?term=TERG_00714). The annotated protein (accession number XP_003238727) identified by InterProScan and ScanProsite domain search tools is 620 amino acid residues long containing a conserved APSES domain (IPR003163) and the residues 135–241. BLASTP searches for StuA orthologs, and multiple sequence alignments of selected orthologs revealed that StuA from *T. rubrum* shared medium percent identities with MSTU1 from *M. grisea* (45 %), Asm-1 from *N. crassa* (45 %), StuA from *A. fumigatus* (50 %), and StuA from *A. nidulans* (50 %), presenting a high percent of identities with StuA orthologs among the dermatophytes. The region comprising the APSES domain was highly conserved among all sequences analyzed (results not shown).

3.2. stuA was upregulated during the growth of T. rubrum in keratin

We analyzed the gene expression profile of *stuA* during the growth of *T. rubrum* in keratin broth, containing water and keratin powder as the sole source of nutrients. Transcriptional analyses by real-time PCR (qRT-PCR) revealed that *stuA* was upregulated in serial time-points during the growth of *T. rubrum* in keratin (Fig. 1).

3.3. Generation of stuA null mutants in T. rubrum

Next, to investigate the functions of the *stuA* gene in *T. rubrum* and its potential involvement in its virulence, we generated the mutant strains by deleting the *stuA* gene, followed by a targeted replacement with the selectable marker hygromycin B phosphotransferase (*hph*) gene. The gene-targeting constructs were generated following the double-joint PCR (Yu et al., 2004) and split marker (Catlett et al., 2003) methodologies with successive PCR rounds (Fig. 2A and B). The constructs were introduced into WT protoplasts, and hygromycin-resistant transformants from independent transformations were obtained and screened. We performed diagnostic PCR and initially identified two putative *stuA* mutants, not amplifying a 143-bp fragment, corresponding to an internal region of *stuA* (Fig. 2C). A second PCR with primers flanking the *stuA* locus amplified a 6.3-kb fragment, in contrast to the 5.6 kb product from the WT, containing the *stuA* gene, confirming the replacement of *stuA* by the *hph* cassette in the putative mutants (Fig. 2D).

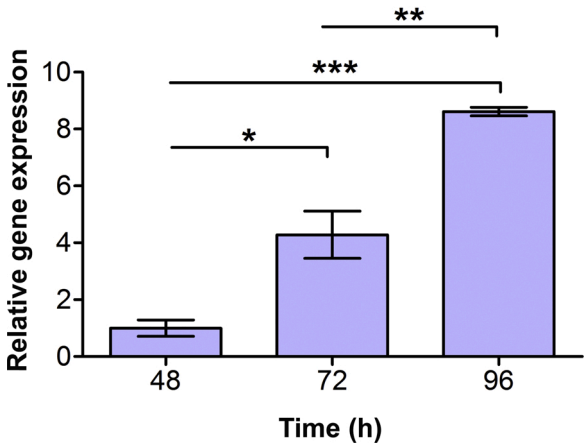

Fig. 1. Transcription profile of *stuA* during the growth of the *T. rubrum* in keratin. Conidia were inoculated in keratin broth, and mycelia were collected in a time-course experiment after 48 h, 72 h, and 96 h of growth at 28 °C. Total RNA was isolated for qRT-PCR analyses. Relative gene expression was calculated using the sample collected at 48 h as the reference sample. Values are the average from three independent experiments, with the respective standard deviations. Statistically significant differences were determined by one-way analysis of variance followed by Bonferroni's multiple comparison tests and are indicated by asterisks (*$p < 0.05$; **$p < 0.01$; ***$p < 0.001$).

Further, Southern hybridization detected DNA fragments of different-sizes, either 6.1 kb in the WT or 2.8 kb in the absence of *stuA*, and confirmed the generation of Δ*stuA*(1) and Δ*stuA*(2) mutant strains (Fig. 2E). Moreover, the Southern hybridization probed with the *hph* cassette confirmed the absence of ectopic integrations of the gene-targeting constructs in Δ*stuA*(1) and Δ*stuA*(2) strains (results not shown).

3.4. Deletion of stuA altered colony growth, morphology, and pigmentation of T. rubrum

We initially compared the growth of the WT, Δ*stuA*(1), and Δ*stuA*(2) strains on various nutritional media. All strains were cultured on solid MEA, SAB, PDA, and MM (Fig. 3). Δ*stuA*(1) and Δ*stuA*(2) were able to grow on all conditions tested. However, the mutant strains presented phenotypic changes compared with the WT strain. The WT strain produced fluffy cotton-like colonies, and the characteristic *T. rubrum* red-brownish pigmentation was evident on the reverse side of the colonies cultured on MEA, SAB, or PDA plates. Unlike the WT strain, the Δ*stuA*(1), and Δ*stuA*(2) mutant strains produced flatter colonies with the wrinkled appearance and creamy-white pigmentation on the reverse side of the plates (Fig. 3A). The mutant strains did not produce the red-brownish pigmentation even after prolonged incubation in tested conditions (not shown). Compared with the WT strain, the mutant strains also displayed delayed radial growth rates (Fig. 3B) and conidia suspensions with altered pigmentation (Fig. 3C).

3.5. StuA is involved in aerial growth and hyphae hydrophobicity in T. rubrum

Because Δ*stuA*(1) and Δ*stuA*(2) mutants produced flatter colonies, we investigated whether deleting *stuA* affected both aerial and invasive hyphae growth. WT colonies cultured on MEA and SAB, presented long and thin aerial hyphae, whereas Δ*stuA*(1) and Δ*stuA*(2) colonies cultured on both media presented shorter aerial hyphae, prominently after growth on MEA. However, all strains exhibited similar invasive growth in the conditions tested (Fig. 4A). Owing to the weak aerial growth, we evaluated whether *stuA* deletion altered the hyphal hydrophobicity. After dropping water on WT, Δ*stuA*(1), and Δ*stuA*(2) colonies, Δ*stuA*(1) and Δ*stuA*(2) cultured on MEA displayed a readily

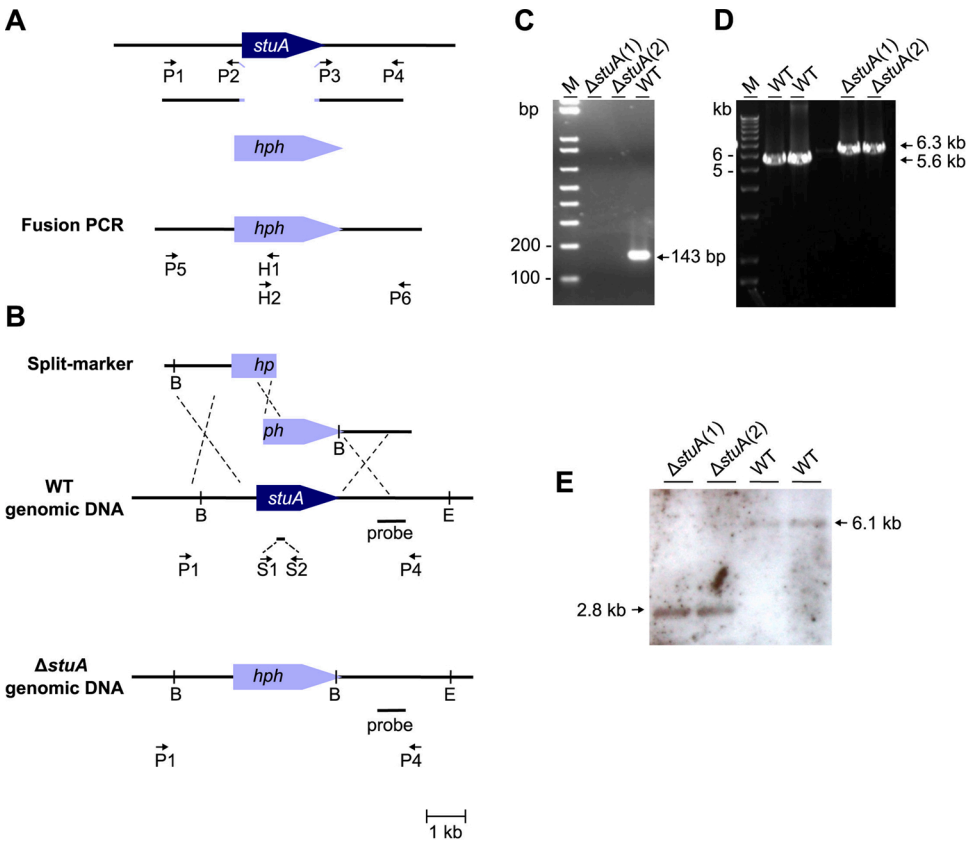

Fig. 2. Generation of *stuA* null mutants in *T. rubrum*. Schematic representation of the construction of Δ*stuA* strains **(A and B)** and molecular analyses **(C to E)**. *stuA* DNA flanking regions were amplified by PCR with primers P1 and P2 and with P3 and P4. Primers P2 and P3 have tails complementary to the *hph* cassette sequence, used as a selectable marker. The flanking fragments and *hph* cassette were mixed and fused by PCR **(A)**. In the following PCR round, the fused product was the template to amplify split-marker fragments with primers P5 and H1 and with H2 and P6. The resulting fragments with an overlapping region were co-transformed into *T. rubrum* wild-type (WT) protoplasts. A triple homologous recombination event resulted in the generation of the Δ*stuA* mutant strains **(B)**. *stuA* Replacement by *hph* cassette was analyzed by PCR with primers S1 and S2 **(C)** and with primers P1 and P4 **(D)** as well as by Southern blot of the digested genomic DNA with EcoRI (E) and BamHI (B) probed with *stuA* fragment **(E)**. DNA molecular size standards (M) and DNA fragment sizes are indicated.

wettable phenotype, and water droplets were immediately soaked into their mycelia but not into WT mycelia (Fig. 4B). This indicated that Δ*stuA*(1) and Δ*stuA*(2) hyphae were more hydrophilic than WT hyphae. When colonies grown on SAB were tested, water droplets remained onto the mycelia of all strains (Fig. 4B). However, the droplets presented increased in surface contact on Δ*stuA*(1) and Δ*stuA*(2) mycelia than on the WT mycelia (Fig. 4C), indicating a reduced hydrophobicity of the *stuA* mutants hyphae. Furthermore, the analysis of *hypA* modulation showed a significant decrease in its transcript levels for mutant strain Δ*stuA*(2) after growing in keratin medium compared to WT strain (Fig. 5).

3.6. StuA is implicated in morphogenesis and germination in T. rubrum

We evaluated the effects of *stuA* deletion on microscopic aspects of hyphae and conidia. Compared with the longer, thinner hyphae, and smaller conidia produced by the WT strain cultured on MEA, the *stuA* mutant strains resulted in an altered phenotype with hypertrophic characteristics. Unlike the WT strain, the Δ*stuA*(1), and Δ*stuA*(2) mutant strains displayed thicker and shorter hyphae and conidia with increased size. In addition, the mutant strains produced hyphae containing abnormal swollen thick-walled regions, resembling chlamydoconidia (Fig. 6A). Moreover, when Δ*stuA*(1) and Δ*stuA*(2) conidia were inoculated in SAB broth, they germinated faster than the WT conidia (Fig. 6B). This feature was also observed when conidia were inoculated on solid medium (not shown).

3.7. Deletion of stuA increased conidia susceptibility to heat-shock and UV light exposure

Next, we evaluated the effect of the phenotypic changes presented by *stuA* mutant conidia on their survival rate subjected to environmental stresses. The results showed that as compared with WT conidia, Δ*stuA*(1) and Δ*stuA*(2) conidia presented increased susceptibility to heat shock and UV light. After the exposure to those stresses, conidia from the mutant strains displayed a more noticeable reduction in viability than those from the WT strain (Fig. 7).

3.8. StuA is involved in keratin degradation

We investigated the possible role of StuA in *T. rubrum* virulence by evaluating the ability of *stuA* mutants to grow on keratinized substrates. Initially, the strains were inoculated on keratin media, containing distilled water and keratin as the sole source of nutrients. Compared with the WT strain, Δ*stuA*(1) and Δ*stuA*(2) strains displayed impaired growth and could not form colonies on solid keratin medium (Fig. 8A). The inoculum of either conidia or mycelia provided identical results (not shown). However, after inoculation into liquid keratin media, all strains (WT, Δ*stuA*(1), and Δ*stuA*(2) mutants) could grow. All strains alkalinized the culture media equally (Fig. 8B) and produced equivalent biomasses (Fig. 8C). We used the crude culture supernatants to quantify keratin degradation by secreted proteases. Compared with the WT strain, Δ*stuA*(1) and Δ*stuA*(2) strains presented a reduction in keratinolytic activities (Fig. 8D).

3.9. Deletion of stuA altered the growth of T. rubrum on human models of infection

To evaluate whether StuA is important for the growth of *T. rubrum* in host microenvironments, we used established human models of nail and skin infections *in vitro* (Grumbt et al., 2013; Peres et al., 2016). Conidia from WT, Δ*stuA*(1), and Δ*stuA*(2) strains were inoculated on *ex vivo* human nail fragments, and the fungal growth was evaluated. We observed a significant increase in conidia size in both the mutant strains, compared to the conidia size in WT strain (Fig. 9A). The WT strain was able to grow and colonize nail fragments completely, unlike the Δ*stuA*

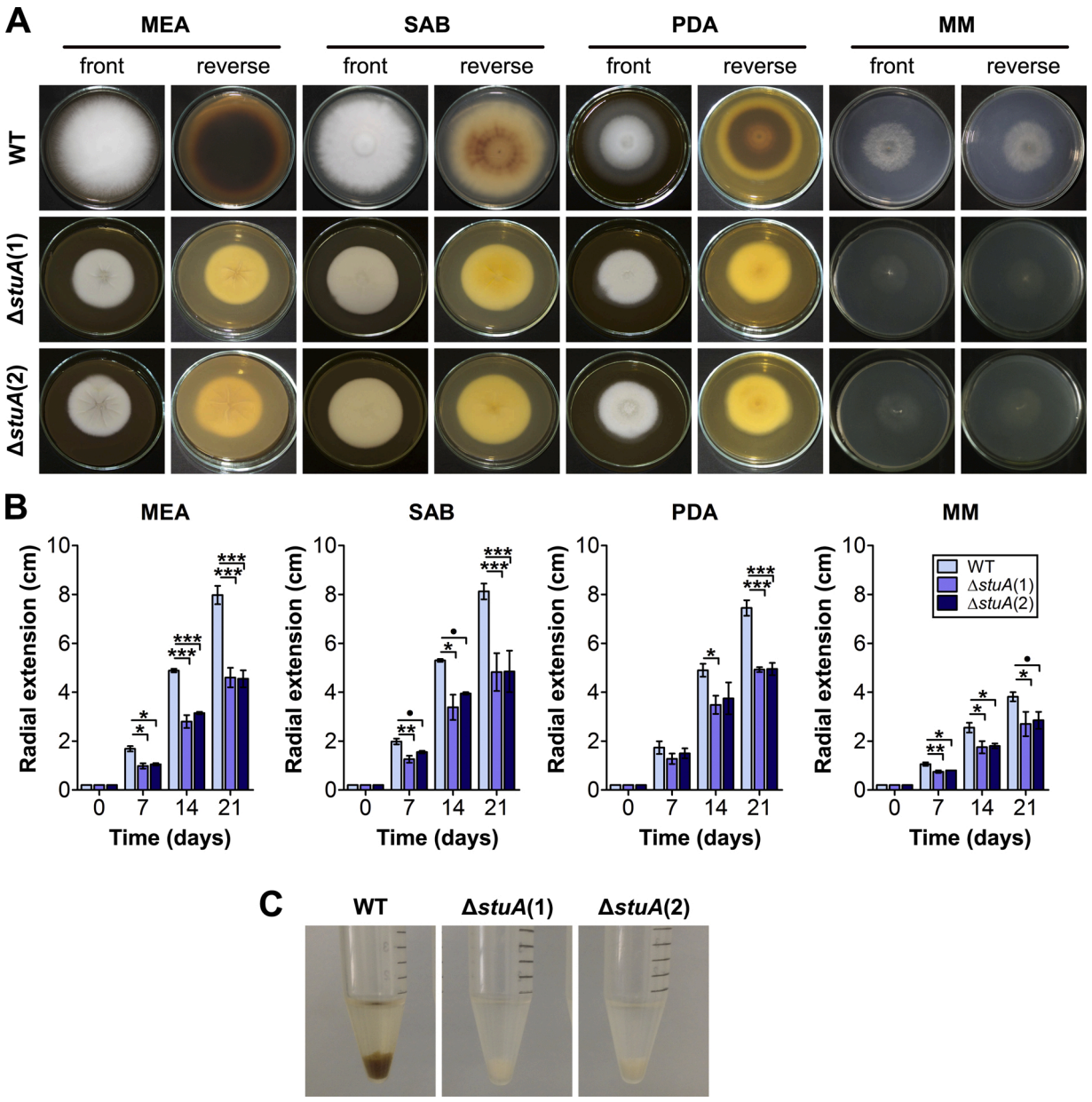

Fig. 3. Colony growth, morphology, and pigmentation of *T. rubrum*. Mycelial plugs from wild-type (WT) or Δ*stuA*(1) and Δ*stuA*(2) mutant strains were inoculated on the center of malt extract (MEA), Sabouraud (SAB), potato dextrose (PDA), or minimal (MM) solid media and incubated at 28 °C. Fungal growth was monitored for 21 days. Front and reverse side of the plates were photographed **(A),** colony radial extension was measured **(B)**, and conidia suspensions were obtained from mycelia grown on MEA **(C)**. All results are representative of three independent experiments. Statistically significant differences were determined by one-way analysis of variance followed by Bonferroni's multiple comparison tests and are indicated ($p^{\cdot} < 0.1$; *$p < 0.05$; **$p < 0.01$; ***$p < 0.001$).

(1) and Δ*stuA*(2) strains, which presented impaired growth (Fig. 9B, upper panels), even after prolonged incubation (not shown). Scanning electron microscopy of nail fragments revealed that adhesion and germination capabilities were not compromised in Δ*stuA*(1) and Δ*stuA* (2) strains (Fig. 9B, lower panels). When conidia were inoculated on *ex vivo* human skin fragments, Δ*stuA*(1) and Δ*stuA*(2) strains displayed reduced growth on that substrate compared with the WT strain (Fig. 9C, upper panels), but adhesion, germination, and skin invasion were not impaired (Fig. 9C, middle and lower panels). As keratinocytes are the predominant cell type of the epidermis and are responsible for the barrier function of the skin, we also evaluated the conidia germination during the interaction with human keratinocytes *in vitro*. Conidia were co-cultured with keratinocytes; after 24 h of interaction, the Δ*stuA*(1) and Δ*stuA*(2) strains displayed a more vigorous development compared with the WT strain (Fig. 10). Tests conducted with the same strains in the RPMI medium ruled out the culture medium itself as causing this effect (results not shown).

4. Discussion

Here, we generated two null mutant strains by the deletion of *stuA* gene in the dermatophyte *T. rubrum* to investigate the role of the APSES transcription factor StuA. The APSES family of transcription factors is unique to fungi and acts as a key regulator of fungal development (Zhao et al., 2015).

The deletion of *stuA* in *T. rubrum* resulted in a dramatic change in the morphology of hyphae and conidia, and flat whitish colonies with decreased radial growth were observed. Delayed colony radial growth has been previously reported in Δ*stuA* mutants of *Fusarium graminearum* and *A. benhamiae* (Lysoe et al., 2011; Krober et al., 2017). Turgor

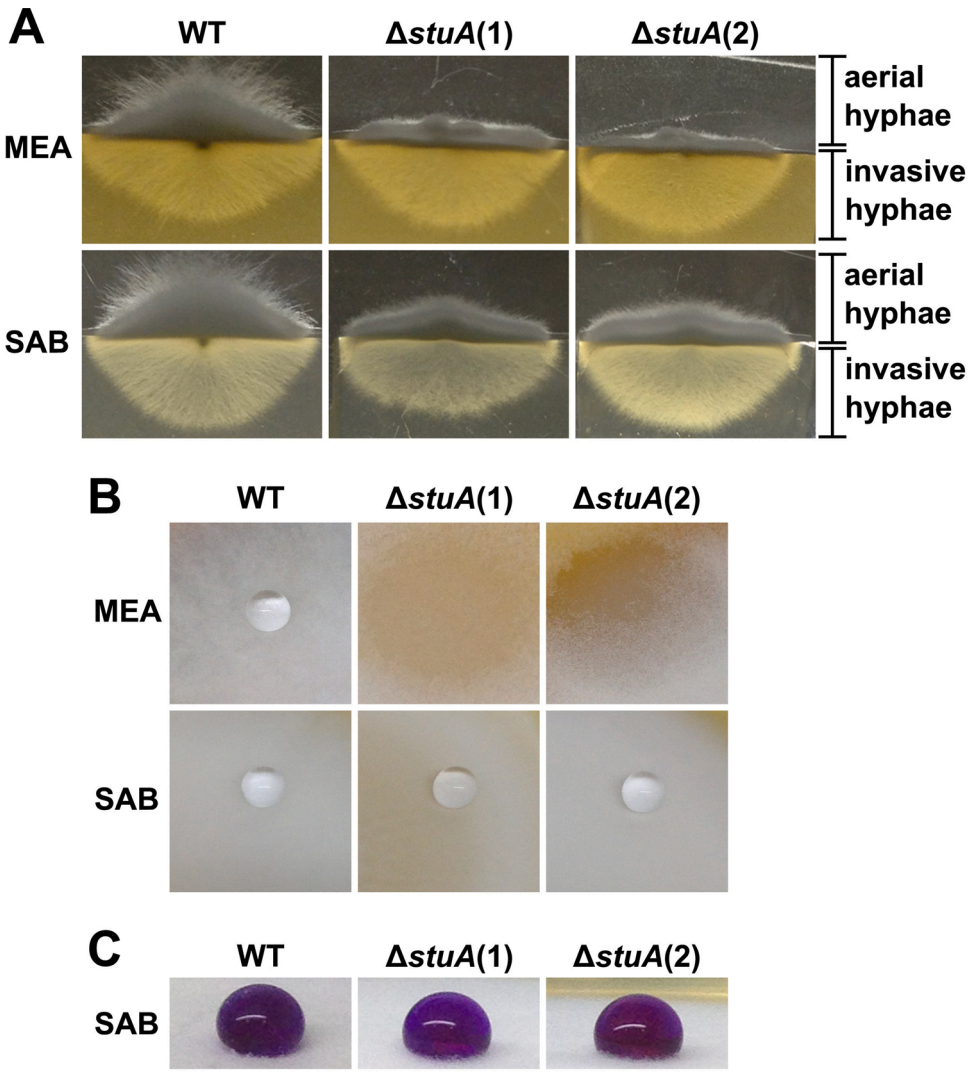

Fig. 4. Aerial and vegetative hyphae and hyphal hydrophobicity of *T. rubrum*. Mycelial plugs from wild-type (WT), ΔstuA(1), and ΔstuA(2) strains were inoculated on malt extract (MEA) or Sabouraud (SAB) solid media. After 5 days at 28 °C, side views of colonies were assessed to analyze aerial and invasive hyphae growth (**A**). After 21 days at 28 °C, hyphal hydrophobicity was tested by placing drops of water (**B**) or water colored with bromophenol blue (**C**) onto mycelia.

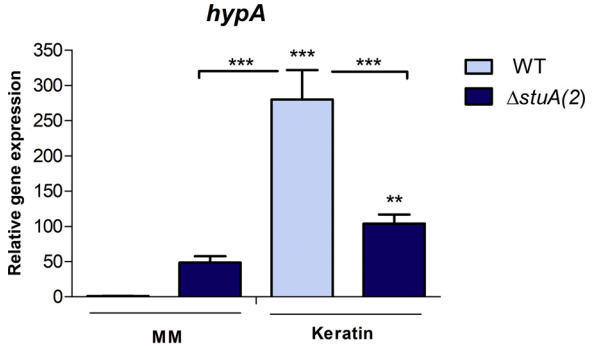

Fig. 5. Transcriptional levels of the *hypA* gene from *T. rubrum*. Relative expression was evaluated by qPCR using minimal medium (MM) as a reference sample. Mycelia from both strains wild type and ΔstuA(2) were inoculated in MM and keratin medium (keratin) for 24 h. Significantly different values are shown by asterisks, and were determined using analysis of variance followed by Tukey's *ad hoc* test (**$P < 0.01$; ***$P < 0.001$).

pressure is the physical force that drives the expansion of the cell wall of growing hypha (Bartnicki-Garcia et al., 2000), and StuA is involved in the maintenance of normal turgor pressure within the appressorium of *G. cingulate* (Tong et al., 2007). Thus, the turgor pressure of cells in the *stuA* mutants of *T. rubrum* may be altered.

Here, we assessed various characteristics of *T. rubrum* Δ*stuA* strains, such as hypertrophy, hyphae thickness, conidia size, as well as the presence of chlamydoconidia. Some fungi produce these structures in response to stresses, including the alterations in osmolarity, temperature, and presence of antifungals (de Oliveira Pereira et al., 2013). Thus, we hypothesized that chlamydoconidia were produced to protect *T. rubrum* from the metabolic stress caused by the *stuA* mutation.

T. rubrum Δ*stuA* mutant strains have also shown a decrease in aerial hyphae growth, as previously described for other fungi (Tong et al., 2007; Lysoe et al., 2011; Krober et al., 2017; Longo et al., 2018; Xie et al., 2019) while displaying an increase in hyphal formation in broth media. These traits correlate to a boost in hydrophilic potential representing their correlation to the differences in the expression levels of hydrophobins, which was confirmed by analysis of the *hypA* gene. However, the different expression levels of hydrophobins might be responsible for other phenomena observed in this work.

The hydrophobins are small and amphiphilic proteins containing eight cysteine residues in a conserved pattern and are restricted to

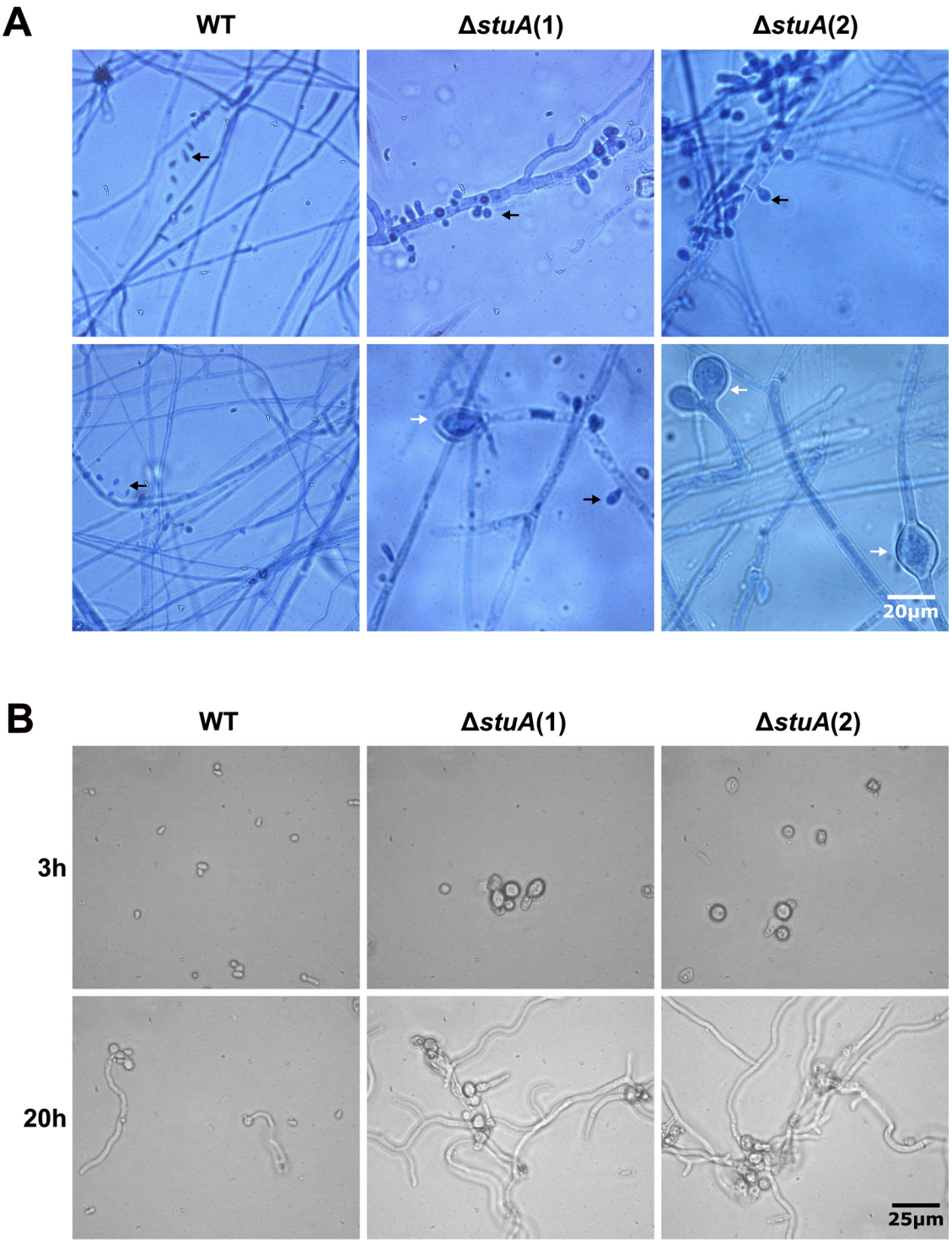

Fig. 6. Microscopic aspects of hyphae, conidia, and germination of *T. rubrum*. Wild-type (WT), Δ*stuA*(1) and Δ*stuA*(2) strains were grown on malt extract agar (MEA) slide culture for 15 days at 28 °C, stained with lactophenol cotton blue, and visualized by light microscopy. Black and white arrows indicate conidia and abnormal swollen regions, respectively **(A)**, WT, Δ*stuA*(1), and Δ*stuA*(2) conidia were inoculated into Sabouraud broth, and germination was evaluated by light microscopy after 3 h and 20 h of incubation **(B)**.

filamentous fungi (Bayry et al., 2012). These proteins are involved in conidia germination, morphogenetic processes, cell wall architecture, fungal attachment to solid supports, and virulence (Wessels, 1997; Whiteford and Spanu, 2001; Fuchs et al., 2004; Quarantin et al., 2019). The hydrophobic coat in the outer layers of conidia and hyphae cell wall plays an essential role in conidia protection against wetting, desiccation, and favors conidia dispersal (Wosten, 2001; Klimes and Dobinson, 2006). Here, we hypothesize that swollen conidia and rapid germination of the mutant strains of *T. rubrum* Δ*stuA* are related to an imbalance in osmoregulation leading to disturbances in metabolism and cell wall construction. The intracellular contents of compatible solutes can also influence the speed of conidia germination (Hallsworth and Magan, 1995). Moreover, fungi can respond to stress by the following mechanisms: reinforcing the cell wall, changing the plasma membrane

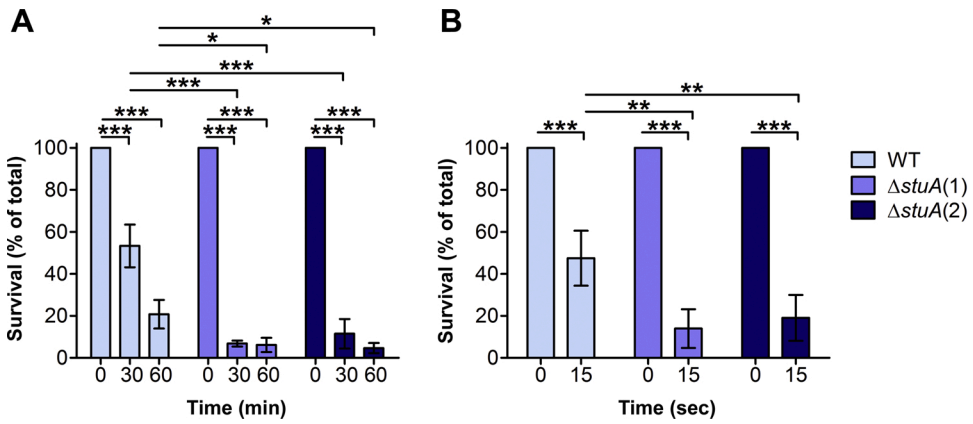

Fig. 7. Susceptibility of *T. rubrum* to heat-shock and UV light exposure. Conidia from wild-type (WT), Δ*stuA*(1), and Δ*stuA*(2) strains were subjected to heat shock at 42 °C for 30 min and 60 min **(A)** or to UV light exposure for 15 s **(B)**. Relative survival was the percentage of colony-forming units (CFUs) after each treatment compared with CFUs before the treatment. Values are the average from three biological replicates from independent experiments with the respective standard deviations. Statistically significant differences were determined by one-way analysis of variance followed by Bonferroni's multiple comparison test and are indicated by asterisks (*p < 0.05; **p < 0.01; ***p < 0.001).

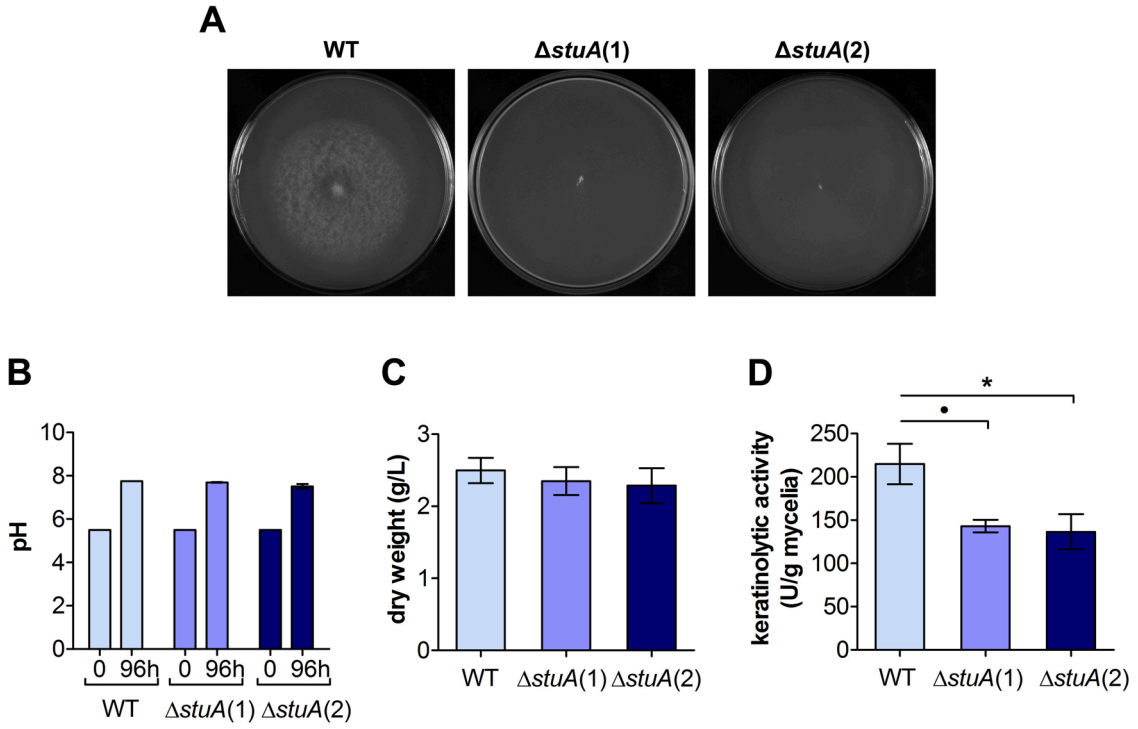

Fig. 8. Growth of *T. rubrum* in keratin and quantification of keratinolytic activity. Wild-type (WT), Δ*stuA*(1), and Δ*stuA*(2) strains were cultivated in both solid and liquid keratin media. For growth on solid medium, mycelial plugs were inoculated on the center of keratin-agar plates, followed by incubation at 28 °C for 21 days **(A)**. For growth in the liquid medium, conidia were inoculated in keratin broth and cultured at 28 °C. After 96 h, each culture was filtered to collect mycelia and culture supernatant. The pH of the culture supernatants was measured **(B)**, mycelial dry weight **(C)**, and the keratinolytic activities of the crude culture supernatants were quantified **(D)**. Values are the average from three biological replicates from independent experiments, with the respective standard deviations. Statistically significant differences were determined by one-way analysis of variance followed by Bonferroni's multiple comparison tests and are indicated (p˙ < 0.1; *p < 0.05).

composition, increasing the carbon flux and generation of energy, among others (Hallsworth, 2018)

Noteworthy, other studies have correlated the cell wall structure/integrity to the signaling pathways such as MAP cell wall integrity pathway and high-osmolarity glycerol (*Hog1*) pathway with hydrophobin and with StuA (Fuchs and Mylonakis, 2009; Moonjely et al., 2018; Cairns et al., 2019). Thus, the cell wall structure/integrity may be related to the metabolism of triacylglycerols, which dictates the fluidity of the plasma membrane, and consequently modulates the cell signaling including the synthesis of high-osmolarity solutes.

Moreover, it has also been shown that the StuA of *A. nidulans* controls the hydrophobin gene induction in response to sugarcane bagasse (Brown et al., 2016). Besides, the association of the hydrophobin with mechanosensing as a response to phytopathogen infection has also been shown in *Lotus japonicus* (Moscatiello et al., 2018). We assessed differences in the pattern of infection in mutant strains under different experimental conditions such as growth on nail fragments, skin, and co-culture with keratinocytes. We strongly believe that these differences might also be affected by the mechanosensing response of these mutant strains. Changes in the conidia and hyphae cell wall coating by hydrophobin are related to the production of aggregate formations and influence the contact surface (Winandy et al., 2018). Besides, the previous findings on a possible change in the central carbon metabolism in Δ*stuA* mutant strains and an attempt to shift the energy metabolism to alternative routes (IpCho et al., 2010) may support our data.

To further characterize the role of StuA mutants of *T. rubrum*, we assessed several virulence traits of StuA, such as keratinolytic enzyme secretion, pigmentation, thermal tolerance, and *ex vivo* interaction with

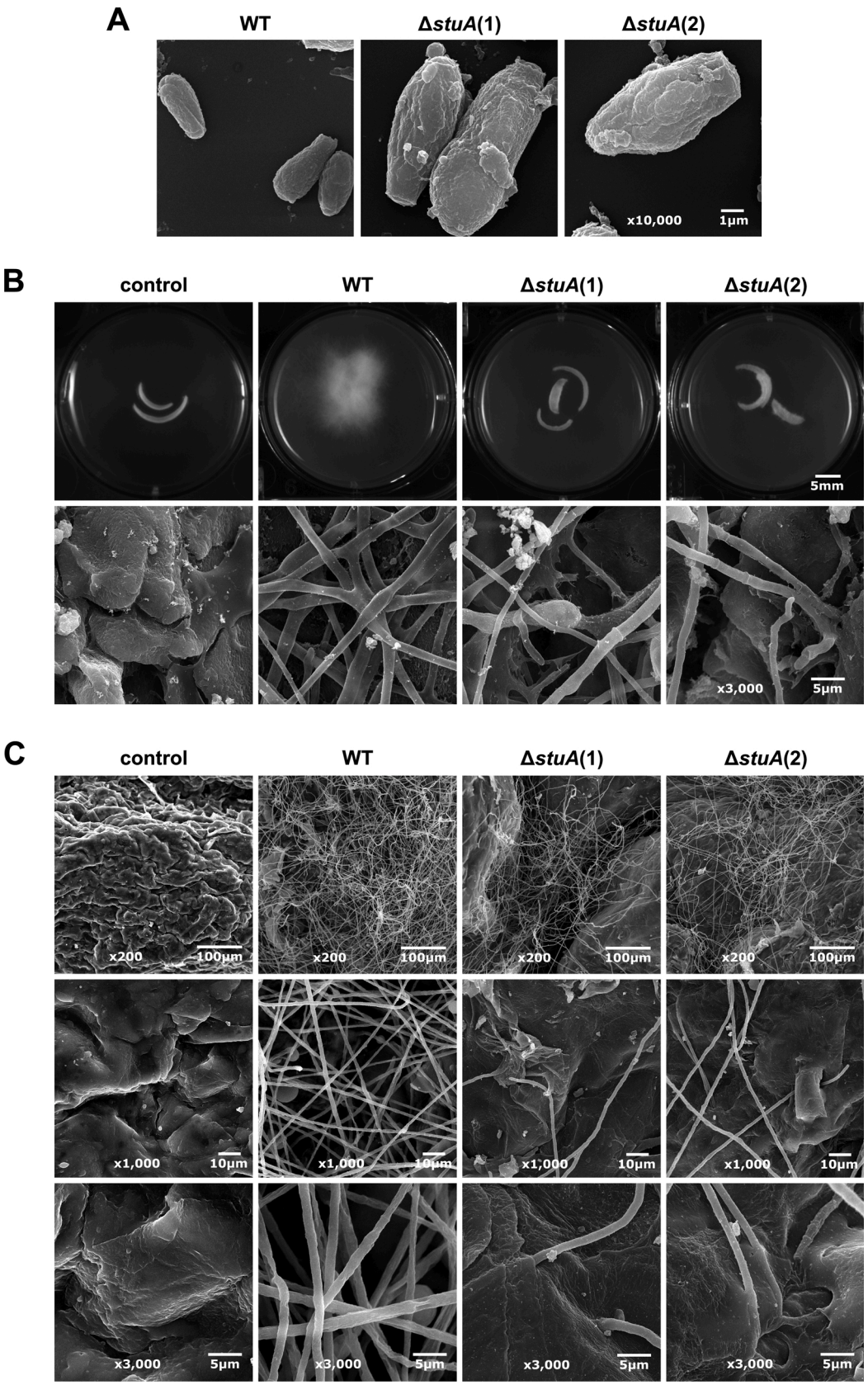

Fig. 9. Growth of *T. rubrum* on human nails and skin. Scanning electron microscopy (SEM) photomicrographs of wild-type (WT), Δ*stuA* (1), and Δ*stuA*(2) conidia used to inoculate human nails and skin *ex vivo* **(A).** Human nail and skin fragments inoculated with conidia were incubated at 28 °C. Nail fragments were photographed after 30 days of incubation **(B, upper panels)** and analyzed by SEM **(B, lower panels)**, and skin fragments were analyzed by SEM after 96 h of incubation **(C).** Controls are nail and skin fragments not inoculated with conidia.

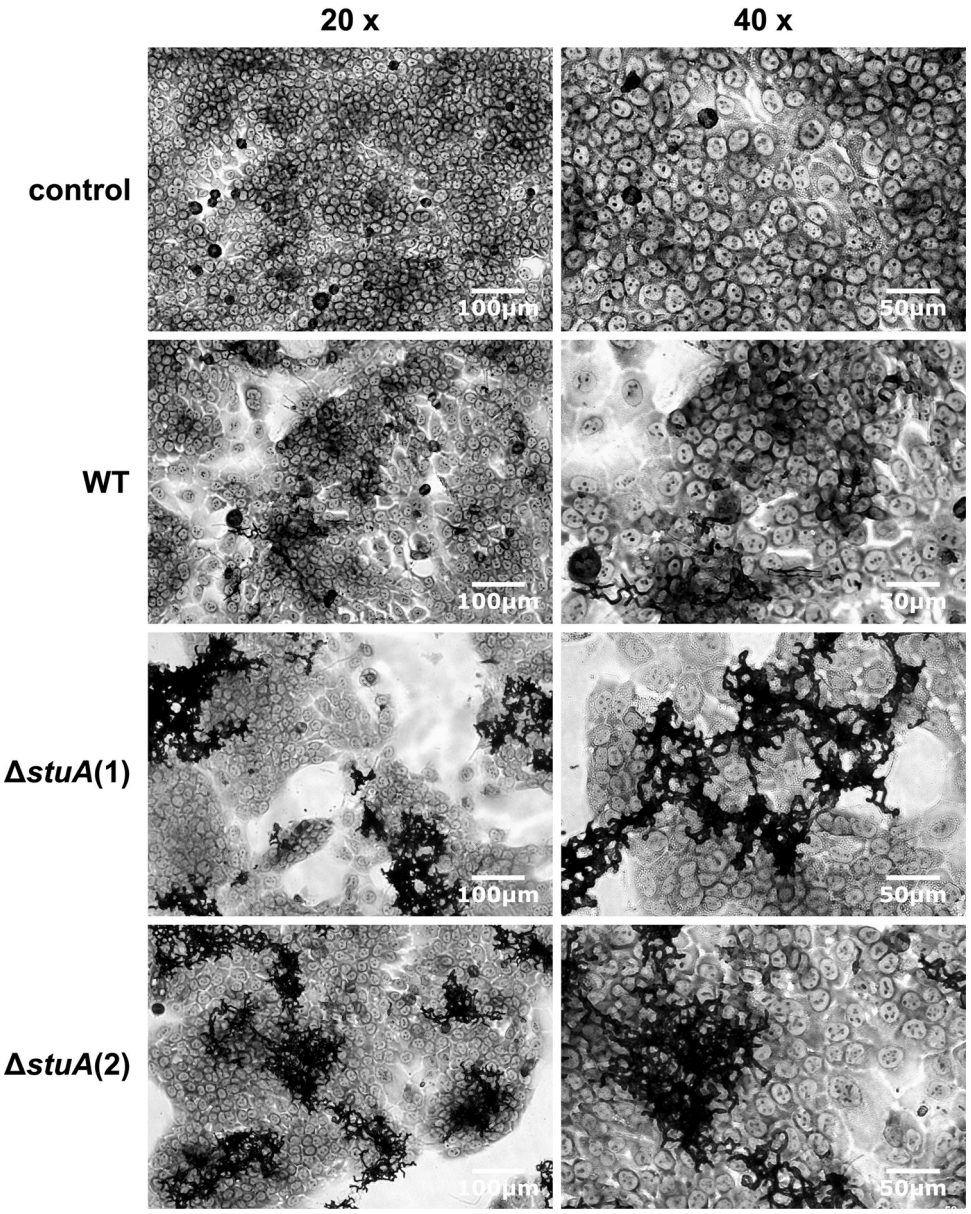

Fig. 10. Co-culture of *T. rubrum* with human keratinocytes. Conidia from wild-type (WT), Δ*stuA*(1), or Δ*stuA*(2) strains were co-cultured with HaCat human keratinocytes at 37 °C for 24 h. After May-Grünwald-Giemsa staining, co-cultures were analyzed by light microscopy imaging. Controls are keratinocytes cultured in the absence of conidia.

human skin and nails, as representative of the host microenvironment.

We observed that *T. rubrum* Δ*stuA* mutants lack the characteristic pigmentation present in the WT strain. It has been previously reported that *T. rubrum* produces xanthomegnin, a mycotoxin, responsible for the characteristic red-brownish color on the reverse side of the colony plates (Wirth, 1965). *T. rubrum* also produces melanin or melanin-like pigments *in vitro* and during skin infections (Youngchim et al., 2011).

Pigmentation has been correlated to stress tolerance upon exposure to UV and higher temperatures (Kawamura et al., 1999; Paolo et al., 2006; Gao et al., 2020), as well as hydrophobin expression (Moonjely et al., 2018). Melanin creates an environment in the cell that favors the accumulation of solutes by generating a high turgor pressure and creating a barrier to glycerol influx/efflux (Foster et al., 2017). Melanin-deficient mutants of *M. oryzae* do not generate cellular turgor pressure in appressoria and are non-pathogenic (Chumley and Valent, 1990), suggesting a relationship between melanin, accumulation of compatible solutes, and virulence. Thus, our results indicate that StuA participates directly or indirectly in these cellular events in *T. rubrum*. Moreover, previous studies have shown that the resistance of ascospores to heat in *Neosartorya fischeri* (*Aspergillus fischeri*) is correlated with intracellular viscosity and the level of compatible solutes (Wyatt et al., 2015).

The secretion of hydrolytic and keratinolytic enzymes contributes to the establishment and survival of the dermatophyte in the host (Monod et al., 2002; Tainwala and Sharma, 2011; Tran et al., 2016; Baumbach et al., 2020). These enzymes are differentially regulated based on the microenvironment and keratin sources available (Staib et al., 2010; Bitencourt et al., 2016; Peres et al., 2016; Tran et al., 2016; Petrucelli et al., 2018). Moreover, a correlation between the keratinolytic activity and disease severity has been previously proposed (Viani et al., 2001). Furthermore, the growth of *T. rubrum* in keratin shows dynamic metabolic modulation involving the metabolism of carbon and nitrogen and increased levels of urea secreted in the culture supernatants that also contribute to keratin degradation (Martins et al., 2020).

Here, we showed that in *T. rubrum* the deletion mutants of*stuA* presented an impairment when grown on skin or nail, and showed a

significant reduction in keratinolytic activity. We speculated that StuA may play a role in keratin degradation and virulence via the regulation of the secretory mechanism. The involvement of StuA in the control of proteolytic activity and virulence was recently reported in the nematophagous *A. oligospora* (Xie et al., 2019). Moreover, the *stuA* mutant of *A. benhamiae* was unable to grow on human hair or nails, suggesting the participation of StuA in the virulence of this dermatophyte (Krober et al., 2017).

The study of the role of a transcription factor such as StuA with pleiotropic functions highlights the conundrums behind transcription factors in fungal pathobiology. Moreover, the *in-silico* analysis conducted to predict potential StuA target genes showed a total of 1,548 genes (about 17 % of total genome of *T. rubrum*) with at least one binding site for this transcription factor (Supplementary Fig. S1). These data strengthened the points covered by our study and showed the involvement of StuA in main representative classes related to oxidation-reduction, phosphorylation, proteolysis, transcription/translation regulation, and carbohydrate metabolism, among others.

5. Conclusion

Collectively our data showed the StuA from *T. rubrum* as a crucial molecular target to be exploited in anti-dermatophytes therapies. Herein we showed the involvement of StuA in many cellular processes, which strengthen the possibility of this transcription factor as a crosstalk mediator regulating different paths to confer adaptive responses and favor fungal-host interaction. Notwithstanding, a depth knowledge about this transcription factor could be achieved using high throughput approaches.

Author contributions

E.A.S.L., N.M.M.-R, and A.R. conceived the study. E.A.S.L. designed and performed most of the laboratory experiments, and assembled the figures. N.T.A.P., and L.G.S. contributed with deletion cassette construction and transformation experiments. L.L. and N.T.A.P. helped with the skin infection experiment. T.A.B. performed co-culture with keratinocytes. T.A.B. and R.A.C. performed some gene expression experiments. E.A.S.L., T.A.B., N.T.A.P., N.M.M.-R., and A.R. wrote the manuscript.

Funding

This work was supported by grants from the Brazilian Agencies: The São Paulo Research Foundation - FAPESP [proc. No. 2019/22596-9, and Fellowships No. 2011/08424-9 to E.A.S.L., No. 2015/23435-8 to T.A.B, No. 2009/08411-4 to N.T.A.P., and No. 2010/15017-8 to L.G.S.]; National Council for Scientific and Technological Development – CNPq [Grants No. 305797/2017-4 and 304989/2017-7]; Coordenação de Aperfeiçoamento de Pessoal de Nível Superior (CAPES) - Finance Code 001; and Fundação de Apoio ao Ensino, Pesquisa e Assistência -FAEPA.

Declaration of Competing Interest

All authors declare that they have no conflict of interest.

Acknowledgments

We thank V. M. de Oliveira, M. Mazucato, and M. D. Martins for technical support, P. R. Sanches for the bioinformatics analysis, and B. A. M. Cantelli for assistance in coculture assays.

Appendix A. Supplementary data

Supplementary material related to this article can be found, in the online version, at doi:https://doi.org/10.1016/j.micres.2020.126592.

References

Aramayo, R., Peleg, Y., Addison, R., Metzenberg, R., 1996. Asm-1+, a *Neurospora crassa* gene related to transcriptional regulators of fungal development. Genetics 144 (3), 991–1003.

Bartnicki-Garcia, S., Bracker, C.E., Gierz, G., Lopez-Franco, R., Lu, H., 2000. Mapping the growth of fungal hyphae: orthogonal cell wall expansion during tip growth and the role of turgor. Biophys. J. 79 (5) https://doi.org/10.1016/S0006-3495(00)76483-6, 2382-90.S0006-3495(00)76483-76486 [pii].

Baumbach, C.M., Michler, J.K., Nenoff, P., Uhrlass, S., Schrodl, W., 2020. Visualising virulence factors: *Trichophyton benhamiaes* subtilisins demonstrated in a guinea pig skin ex vivo model. Mycoses, 10.1111/myc.13136.

Bayry, J., Aimanianda, V., Guijarro, J.I., Sunde, M., Latge, J.P., 2012. Hydrophobins–unique fungal proteins. PLoS Pathog. 8 (5) e1002700.10.1371/journal.ppat.1002700 PPATHOGENS-D-12-00347 [pii].

Bitencourt, T.A., Macedo, C., Franco, M.E., Assis, A.F., Komoto, T.T., Stehling, E.G., Beleboni, R.O., Malavazi, I., Marins, M., Fachin, A.L., 2016. Transcription profile of *Trichophyton rubrum* conidia grown on keratin reveals the induction of an adhesin-like protein gene with a tandem repeat pattern. BMC Genomics 17 (14). https://doi.org/10.1186/s12864-016-2567-2568.

Bitencourt, T.A., Lang, E.A.S., Sanches, P.R., Peres, N.T.A., Oliveira, V.M., Fachin, A.L., Rossi, A., Martinez-Rossi, N.M., 2020. HacA governs virulence traits and adaptive stress responses in *Trichophyton rubrum*. Front. Microbiol. 11 (193), 10.3389/fmicb.2020.00193.

Brown, N.A., Ries, L.N.A., Reis, T.F., Rajendran, R., dos Santos, R.A.C., Ramage, G., Riano-Pachon, D.M., Goldman, G.H., 2016. RNAseq reveals hydrophobins that are involved in the adaptation of *Aspergillus nidulans* to lignocellulose. Biotech. Biofuels 9. https://doi.org/10.1186/S13068-016-0558-2. Artn 145.

Cairns, T.C., Zheng, X., Zheng, P., Sun, J., Meyer, V., 2019. Moulding the mould: understanding and reprogramming filamentous fungal growth and morphogenesis for next generation cell factories. Biotechnol. Biofuels 12 (77), 10.1186/s13068-019-1400-1404 1400 [pii].

Catlett, N.L., Lee, B., Yoder, O.C., Turgeon, B.G., 2003. Split-marker recombination for efficient targeted deletion of fungal genes. Fungal Genet. Newsl. 50, 9–11.

Chumley, F.G., Valent, B., 1990. Genetic-analysis of melanin-deficient, nonpathogenic mutants of *Magnaporthe-Grisea*. Mol. Plant Microbe Interact. 3 (3), 135–143. https://doi.org/10.1094/Mpmi-3-135.

Cove, D.J., 1966. The induction and repression of nitrate reductase in the fungus *Aspergillus nidulans*. Biochim. Biophys. Acta 113 (1), 51–56.

de Oliveira Pereira, F., Mendes, J.M., de Oliveira Lima, E., 2013. Investigation on mechanism of antifungal activity of eugenol against *Trichophyton rubrum*. Med. Mycol. 51 (5), 507–513. https://doi.org/10.3109/13693786.2012.742966.

Duek, L., Kaufman, G., Ulman, Y., Berdicevsky, I., 2004. The pathogenesis of dermatophyte infections in human skin sections. J. Infect. 48 (2), 175–180.

Dutton, J.R., Johns, S., Miller, B.L., 1997. StuAp is a sequence-specific transcription factor that regulates developmental complexity in *Aspergillus nidulans*. EMBO J. 16 (18), 5710–5721. https://doi.org/10.1093/emboj/16.18.5710.

Ferreira-Nozawa, M.S., Silveira, H.C.S., Ono, C.J., Fachin, A.L., Rossi, A., Martinez-Rossi, N.M., 2006. The pH signaling transcription factor PacC mediates the growth of *Trichophyton rubrum* on human nail *in vitro*. Med. Mycol. 44 (7), 641–645.

Foster, A.J., Ryder, L.S., Kershaw, M.J., Talbot, N.J., 2017. The role of glycerol in the pathogenic lifestyle of the rice blast fungus *Magnaporthe oryzae*. Environ. Microbiol. 19 (3), 1008–1016. https://doi.org/10.1111/1462-2920.13688.

Fuchs, B.B., Mylonakis, E., 2009. Our paths might cross: the role of the fungal cell wall integrity pathway in stress response and cross talk with other stress response pathways. Eukaryot. Cell 8 (11), 1616–1625.

Fuchs, U., Czymmek, K.J., Sweigard, J.A., 2004. Five hydrophobin genes in *Fusarium verticillioides* include two required for microconidial chain formation. Fungal Genet. Biol. 41 (9), 852–864, 10.1016/j.fgb.2004.04.004 S1087184504000672 [pii].

Gao, P., Jin, K., Xia, Y., 2020. The phosphatase gene MaCdc14 negatively regulates UV-B tolerance by mediating the transcription of melanin synthesis-related genes and contributes to conidiation in *Metarhizium acridum*. Curr. Genet. 66 (1), 141–153. https://doi.org/10.1007/s00294-019-01008-3.

Gimeno, C.J., Fink, G.R., 1994. Induction of pseudohyphal growth by overexpression of PHD1, a *Saccharomyces cerevisiae* gene related to transcriptional regulators of fungal development. Mol. Cell. Biol. 14 (3), 2100–2112. https://doi.org/10.1128/mcb.14.3.2100.

Grumbt, M., Monod, M., Yamada, T., Hertweck, C., Kunert, J., Staib, P., 2013. Keratin degradation by dermatophytes relies on cysteine dioxygenase and a sulfite efflux pump. J. Invest. Dermatol. 133 (6), 1550–1555.

Hallsworth, J.E., 2018. Stress-free microbes lack vitality. Fungal Biol. 122 (6), 379–385. S1878-6146(18)30064-3 [pii] 10.1016/j.funbio.2018.04.003.

Hallsworth, J.E., Magan, N., 1995. Manipulation of intracellular glycerol and erythritol enhances germination of conidia at low water availability. Microbiology 141 (Pt 5), 1109–1115. https://doi.org/10.1099/13500872-141-5-1109.

Harris, J.L., 1986. Modified method for fungal slide culture. J. Clin. Microbiol. 24 (3), 460–461. https://doi.org/10.1128/JCM.24.3.460-461.1986.

Heddergott, C., Bruns, S., Nietzsche, S., Leonhardt, I., Kurzai, O., Kniemeyer, O., Brakhage, A.A., 2012. The *Arthroderma benhamiae* hydrophobin HypA mediates hydrophobicity and influences recognition by human immune effector cells. Eukaryot. Cell 11 (5), 673–682.

Hogan, L.H., Klein, B.S., Levitz, S.M., 1996. Virulence factors of medically important fungi. Clin. Microbiol. Rev. 9 (4), 469–488.

IpCho, S.V., Tan, K.C., Koh, G., Gummer, J., Oliver, R.P., Trengove, R.D., Solomon, P.S., 2010. The transcription factor StuA regulates central carbon metabolism, mycotoxin production, and effector gene expression in the wheat pathogen *Stagonospora*

nodorum. Eukaryot. Cell 9 (7). https://doi.org/10.1128/EC.00064-10, 1100-8. EC.00064-10 [pii].
Jacob, T.R., Peres, N.T.A., Persinoti, G.F., Silva, L.G., Mazucato, M., Rossi, A., Martinez-Rossi, N.M., 2012. *rpb2* is a reliable reference gene for quantitative gene expression analysis in the dermatophyte *Trichophyton rubrum*. Med. Mycol. 50 (4), 368–377. https://doi.org/10.3109/13693786.2011.616230.
Jacob, T.R., Peres, N.T.A., Martins, M.P., Lang, E.A., Sanches, P.R., Rossi, A., Martinez-Rossi, N.M., 2015. Heat shock protein 90 (Hsp90) as a molecular target for the development of novel drugs against the dermatophyte *Trichophyton rubrum*. Front. Microbiol. 6 (10).
Kawamura, C., Tsujimoto, T., Tsuge, T., 1999. Targeted disruption of a melanin biosynthesis gene affects conidial development and UV tolerance in the Japanese pear pathotype of *Alternaria alternata*. Mol. Plant Microbe Interact. 12 (1), 59–63. https://doi.org/10.1094/MPMI.1999.12.1.59.
Klimes, A., Dobinson, K.F., 2006. A hydrophobin gene, VDH1, is involved in microsclerotial development and spore viability in the plant pathogen *Verticillium dahliae*. Fungal Genet. Biol. 43 (4), 283–294. S1087-1845(05)00181-00187 [pii] 10.1016/j.fgb.2005.12.006.
Komoto, T.T., Bitencourt, T.A., Silva, G., Beleboni, R.O., Marins, M., Fachin, A.L., 2015. Gene expression response of *Trichophyton rubrum* during coculture on keratinocytes exposed to antifungal agents. Evid. Complement. Alternat. Med. 2015: 180535.10.1155/2015/180535.
Krober, A., Etzrodt, S., Bach, M., Monod, M., Kniemeyer, O., Staib, P., Brakhage, A.A., 2017. The transcriptional regulators SteA and StuA contribute to keratin degradation and sexual reproduction of the dermatophyte *Arthroderma benhamiae*. Curr. Genet. 63 (1), 103–116. https://doi.org/10.1007/s00294-016-0608-0.
Livak, K.J., Schmittgen, T.D., 2001. Analysis of relative gene expression data using real-time quantitative PCR and the 2(-Delta Delta C(T)) Method. Methods 25 (4), 402–408.
Longo, L.V.G., Ray, S.C., Puccia, R., Rappleye, C.A., 2018. Characterization of the APSES-family transcriptional regulators of *Histoplasma capsulatum*. FEMS Yeast Res. 18 (8), 5067870 [pii] 10.1093/femsyr/foy087.
Lysoe, E., Pasquali, M., Breakspear, A., Kistler, H.C., 2011. The transcription factor FgStuAp influences spore development, pathogenicity, and secondary metabolism in *Fusarium graminearum*. Mol. Plant Microbe Interact. 24 (1), 54–67.
Martinez-Rossi, N.M., Persinoti, G.F., Peres, N.T.A., Rossi, A., 2012. Role of pH in the pathogenesis of dermatophytoses. Mycoses 55 (5), 381–387. https://doi.org/10.1111/j.1439-0507.2011.02162.x.
Martinez-Rossi, N.M., Peres, N.T., Rossi, A., 2017. Pathogenesis of dermatophytosis: sensing the host tissue. Mycopathologia 182 (1–2), 215–227. https://doi.org/10.1007/s11046-016-0057-0059.
Martins, M.P., Rossi, A., Sanches, P.R., Bortolossi, J.C., Martinez-Rossi, N.M., 2020. Comprehensive analysis of the dermatophyte *Trichophyton rubrum* transcriptional profile reveals dynamic metabolic modulation. Biochem. J. 477 (5), 873–885. https://doi.org/10.1042/Bcj20190868.
Mehul, B., Gu, Z., Jomard, A., Laffet, G., Feuilhade, M., Monod, M., 2016. Sub6 (Tri r 2), an onychomycosis marker revealed by proteomics analysis of *trichophyton rubrum* secreted proteins in patient nail samples. J. Invest. Dermatol. 136 (1), 331–333. S0022-202X(15)00018-4 [pii] 10.1038/JID.2015.367.
Monod, M., Capoccia, S., Lechenne, B., Zaugg, C., Holdom, M., Jousson, O., 2002. Secreted proteases from pathogenic fungi. Int. J. Med. Microbiol. 292 (5-6), 405–419.
Moonjely, S., Keyhani, N.O., Bidochka, M.J., 2018. Hydrophobins contribute to root colonization and stress responses in the rhizosphere-competent insect pathogenic fungus *Beauveria bassiana*. Microbiology 164 (4), 517–528. https://doi.org/10.1099/mic.0.000644.
Moscatiello, R., Sello, S., Ruocco, M., Barbulova, A., Cortese, E., Nigris, S., Baldan, B., Chiurazzi, M., Mariani, P., Lorito, M., Navazio, L., 2018. The hydrophobin HYTLO1 secreted by the biocontrol fungus *Trichoderma longibrachiatum* triggers a NAADP-Mediated calcium signalling pathway in *Lotus japonicus*. Int. J. Mol. Sci. 19 (9) ijms19092596 [pii] 10.3390/ijms19092596.
Nishimura, M., Fukada, J., Moriwaki, A., Fujikawa, T., Ohashi, M., Hibi, T., Hayashi, N., 2009. Mstu1, an APSES transcription factor, is required for appressorium-mediated infection in *Magnaporthe grisea*. Biosci. Biotechnol. Biochem. 73 (8), 1779–1786. https://doi.org/10.1271/bbb.90146.
Paolo Jr., W.F., Dadachova, E., Mandal, P., Casadevall, A., Szaniszlo, P.J., Nosanchuk, J. D., 2006. Effects of disrupting the polyketide synthase gene WdPKS1 in *Wangiella* [*Exophiala*] *dermatitidis* on melanin production and resistance to killing by antifungal compounds, enzymatic degradation, and extremes in temperature. BMC Microbiol. 6 (55), 1471-2180-6-55 [pii] 10.1186/1471-2180-6-55.
Peres, N.T.A., Silva, L.G., Santos Rda, S., Jacob, T.R., Persinoti, G.F., Rocha, L.B., Falcao, J.P., Rossi, A., Martinez-Rossi, N.M., 2016. In vitro and ex vivo infection models help assess the molecular aspects of the interaction of *Trichophyton rubrum* with the host milieu. Med. Mycol. 54 (4), 420–427.
Petrucelli, M.F., Peronni, K., Sanches, P.R., Komoto, T.T., Matsuda, J.B., Silva Junior, W. A.D., Beleboni, R.O., Martinez-Rossi, N.M., Marins, M., Fachin, A.L., 2018. Dual RNA-Seq analysis of *Trichophyton rubrum* and HaCat keratinocyte Co-culture highlights important genes for fungal-host interaction. Genes (Basel) 9 (7) genes9070362 [pii] 10.3390/genes9070362.
Quarantin, A., Hadeler, B., Kroger, C., Schafer, W., Favaron, F., Sella, L., Martinez-Rocha, A.L., 2019. Different hydrophobins of *Fusarium graminearum* are involved in hyphal growth, attachment, water-air interface penetration and plant infection. Front. Microbiol. 10 (751) https://doi.org/10.3389/fmicb.2019.00751.
Ramage, G., VandeWalle, K., Lopez-Ribot, J.L., Wickes, B.L., 2002. The filamentation pathway controlled by the Efg1 regulator protein is required for normal biofilm formation and development in *Candida albicans*. Fems Microbiol. Lett. 214 (1), 95–100. Pii S0378-1097(02)00853-00854 Doi 10.1111/J.1574-6968.2002.Tb11330.X.
Sheppard, D.C., Doedt, T., Chiang, L.Y., Kim, H.S., Chen, D., Nierman, W.C., Filler, S.G., 2005. The *Aspergillus fumigatus* StuA protein governs the up-regulation of a discrete transcriptional program during the acquisition of developmental competence. Mol. Biol. Cell 16 (12). https://doi.org/10.1091/mbc.e05-07-0617, 5866-79.E05-07-0617 [pii].
Sonneborn, A., Bockmuhl, D.P., Ernst, J.F., 1999. Chlamydospore formation in *Candida albicans* requires the Efg1p morphogenetic regulator. Infect. Immun. 67 (10), 5514-7.10.1128/IAI.67.10.5514-5517.1999.
Srikantha, T., Tsai, L.K., Daniels, K., Soll, D.R., 2000. EFG1 null mutants of *Candida albicans* switch but cannot express the complete phenotype of white-phase budding cells. J. Bacteriol. 182 (6), 1580–1591. https://doi.org/10.1128/jb.182.6.1580-1591, 2000.
Staib, P., Zaugg, C., Mignon, B., Weber, J., Grumbt, M., Pradervand, S., Harshman, K., Monod, M., 2010. Differential gene expression in the pathogenic dermatophyte *Arthroderma benhamiae* in vitro versus during infection. Microbiology 156 (Pt 3), 884–895, 156(Pt 3):884-95.mic.0.033464-0 [pii] 10.1099/mic.0.033464-0.
Stoldt, V.R., Sonneborn, A., Leuker, C.E., Ernst, J.F., 1997a. Efg1p, an essential regulator of morphogenesis of the human pathogen *Candida albicans*, is a member of a conserved class of bHLH proteins regulating morphogenetic processes in fungi. EMBO J. 16 (8), 1982–1991.
Stoldt, V.R., Sonneborn, A., Leuker, C.E., Ernst, J.F., 1997b. Efg1p, an essential regulator of morphogenesis of the human pathogen *Candida albicans*, is a member of a conserved class of bHLH proteins regulating morphogenetic processes in fungi. EMBO J. 16 (8), 1982–1991. https://doi.org/10.1093/emboj/16.8.1982.
Tainwala, R., Sharma, Y., 2011. Pathogenesis of dermatophytoses. Indian J. Dermatol. 56 (3), 259–261, 10.4103/0019-5154.82476 IJD-56-259 [pii].
Tong, X., Zhang, X., Plummer, K.M., Stowell, K.M., Sullivan, P.A., Farley, P.C., 2007. GcSTUA, an APSES transcription factor, is required for generation of appressorial turgor pressure and full pathogenicity of *Glomerella cingulata*. Mol. Plant Microbe Interact. 20 (9), 1102-11.10.1094/MPMI-20-9-1102.
Tran, V.D., De Coi, N., Feuermann, M., Schmid-Siegert, E., Bagut, E.T., Mignon, B., Waridel, P., Peter, C., Pradervand, S., Pagni, M., Monod, M., 2016. RNA sequencing-based genome reannotation of the dermatophyte *Arthroderma benhamiae* and characterization of its secretome and whole gene expression profile during infection. mSystems 1 (4), 10.1128/mSystems.00036-16 mSystems00036-16 [pii].
Vermout, S., Tabart, J., Baldo, A., Mathy, A., Losson, B., Mignon, B., 2008. Pathogenesis of dermatophytosis. Mycopathologia 166 (5-6), 267–275.
Viani, F.C., Dos Santos, J.I., Paula, C.R., Larson, C.E., Gambale, W., 2001. Production of extracellular enzymes by *Microsporum canis* and their role in its virulence. Med. Mycol. 39 (5), 463–468. https://doi.org/10.1080/mmy.39.5.463.468.
Wessels, J.G.H., 1997. Hydrophobins: proteins that change the nature of the fungal surface. Adv. Microb. Physiol. 38, 1–45.
Whiteford, J.R., Spanu, P.D., 2001. The hydrophobin HCf-1 of *Cladosporium fulvum* is required for efficient water-mediated dispersal of conidia. Fungal Genet. Biol. 32 (3), 159–168, 10.1006/fgbi.2001.1263 S1087-1845(01)91263-0 [pii].
Winandy, L., Hilpert, F., Schlebusch, O., Fischer, R., 2018. Comparative analysis of surface coating properties of five hydrophobins from *Aspergillus nidulans* and *Trichoderma reseei*. Sci. Rep. 8 (1), 12033, 10.1038/s41598-018-29749-0.
Wirth, J.C.B., T.E, Anand, S.R., 1965. The isolation of xanthomegnin from several strains of the dermatophyte, *Trichophyton rubrum*. Phytochemistry 4 (3), 505–509, 10.1016/S0031-9422(00)86204-4.
Wosten, H.A., 2001. Hydrophobins: multipurpose proteins. Annu. Rev. Microbiol. 55, 625–646, 10.1146/annurev.micro.55.1.625 55/1/625 [pii].
Wu, J., Miller, B.L., 1997. Aspergillus asexual reproduction and sexual reproduction are differentially affected by transcriptional and translational mechanisms regulating stunted gene expression. Mol. Cell. Biol. 17 (10), 6191–6201, 10.1128/mcb.17.10.6191.
Wyatt, T.T., Golovina, E.A., van Leeuwen, R., Hallsworth, J.E., Wosten, H.A., Dijksterhuis, J., 2015. A decrease in bulk water and mannitol and accumulation of trehalose and trehalose-based oligosaccharides define a two-stage maturation process towards extreme stress resistance in ascospores of *Neosartorya fischeri* (*Aspergillus fischeri*). Environ. Microbiol. 17 (2), 383–394. https://doi.org/10.1111/1462-2920.12557.
Xie, M.H., Wang, Y.C., Tang, L.Y., Yang, L., Zhou, D.X., Li, Q., Niu, X.M., Zhang, K.Q., Yang, J.K., 2019. AoStuA, an APSES transcription factor, regulates the conidiation, trap formation, stress resistance and pathogenicity of the nematode-trapping fungus *Arthrobotrys oligospora*. Environ. Microbiol. 21 (12), 4648–4661. https://doi.org/10.1111/1462-2920.14785.
Youngchim, S., Pornsuwan, S., Nosanchuk, J.D., Dankai, W., Vanittanakom, N., 2011. Melanogenesis in dermatophyte species in vitro and during infection. Microbiology 157 (Pt 8), 2348–2356. https://doi.org/10.1099/mic.0.047928-0.
Yu, J.H., Hamari, Z., Han, K.H., Seo, J.A., Reyes-Dominguez, Y., Scazzocchio, C., 2004. Double-joint PCR: a PCR-based molecular tool for gene manipulations in filamentous fungi. Fungal Genet. Biol. 41 (11), 973–981. S1087-1845(04)00118-5 [pii] 10.1016/j.fgb.2004.08.001.
Zhao, Y., Su, H., Zhou, J., Feng, H., Zhang, K.Q., Yang, J., 2015. The APSES family proteins in fungi: characterizations, evolution and functions. Fungal Genet. Biol. 81 https://doi.org/10.1016/j.fgb.2014.12.003, 271-80.S1087-1845(14)00218-7 [pii].